Available online at www.sciencedirect.com
SCIENCE DIRECT®
Molecular Phylogenetics and Evolution 37 (2005) 178–191
MOLECULAR PHYLOGENETICS AND EVOLUTION
www.elsevier.com/locate/ympev

Molecular phylogenetics and evolution of turtles

James G. Krenz [a,1], Gavin J.P. Naylor [a,2], H. Bradley Shaffer [b], Fredric J. Janzen [a,*]

[a] Department of Ecology, Evolution, and Organismal Biology, Iowa State University, Ames, IA 50011-1020, USA
[b] Section of Evolution and Ecology and Center for Population Biology, University of California, Davis, CA 95616, USA

Received 10 November 2004; revised 1 April 2005
Available online 16 June 2005

Abstract

Turtles are one of Earth's most instantly recognizable life forms, distinguished for over 200 million years in the fossil record. Even so, key nodes in the phylogeny of turtles remain uncertain. To address this issue, we sequenced >90% of the nuclear recombination activase gene 1 (RAG-1) for 24 species representing all modern turtle families. RAG-1 exhibited negligible saturation and base composition bias, and extensive base composition homogeneity. Most of the relationships suggested by prior phylogenetic analyses were also supported by RAG-1 and, for at least two critical nodes, with a much higher level of support. RAG-1 also indicates that the enigmatic Platysternidae and Chelydridae, often considered sister taxa based on morphological evidence, are not closely related, although their precise phylogenetic placement in the turtle tree is still unresolved. Although RAG-1 is phylogenetically informative, our research revealed fundamental conflicts among analytical methods for estimating phylogenetic hypotheses. Maximum parsimony analyses of RAG-1 alone and in combination with two mitochondrial genes suggest the earliest phylogenetic splits separating into three basal branches, the pig-nosed turtles (Carettochelyidae), the softshell turtles (Trionychidae), and a clade comprising all remaining extant turtles. Maximum likelihood and Bayesian analyses group Carettochelyidae and Trionychidae (= Trionychoidae) in their more traditional location as the sister taxon to all other hidden-necked turtles, collectively forming the Cryptodira. Our research highlights the utility of molecular data in identifying issues of character homology in morphological datasets, while shedding valuable light on the biodiversity of a globally imperiled taxon.
© 2005 Elsevier Inc. All rights reserved.

Keywords: Evolution; Molecular phylogeny; RAG-1; Turtles

1. Introduction

Turtles have a long and successful evolutionary history (Ernst and Barbour, 1989; Gaffney, 1990). Morphological characters of fossil and extant taxa have long been used to unite turtles as a monophyletic group and to resolve the phylogenetic positions of species (Gaffney, 1984; Gaffney and Meylan, 1988; Gaffney et al., 1991). Molecular approaches have recently been brought to bear on this subject as well, generally providing stronger statistical support for the arrangements identified from morphology alone (Fig. 1; Fujita et al., 2004; Shaffer et al., 1997). Nonetheless, major nodes in the phylogeny of turtles remain uncertain despite a large available data set of mitochondrial DNA (mtDNA), nuclear DNA (nuDNA), and morphological characters (Fujita et al., 2004; Shaffer et al., 1997). These ambiguous relationships obscure insight into the tempo and mode of diversification among major chelonian groups (although progress is being made, see Near et al., 2005), which is important both for understanding the tree of life and for effective

* Corresponding author. Fax: +1 515 294 1337.
E-mail address: fjanzen@iastate.edu (F.J. Janzen).
[1] Present address: USDA/ARS Aquaculture Genetics, Oregon State University-Hatfield Marine Science Center, 2030 SE Marine Science Drive, Newport, OR 97365, USA.
[2] Present address: School of Computational Science and Instructional Technology, Florida State University, Tallahassee, FL 32306-4120, USA.

1055-7903/$ - see front matter © 2005 Elsevier Inc. All rights reserved.
doi:10.1016/j.ympev.2005.04.027

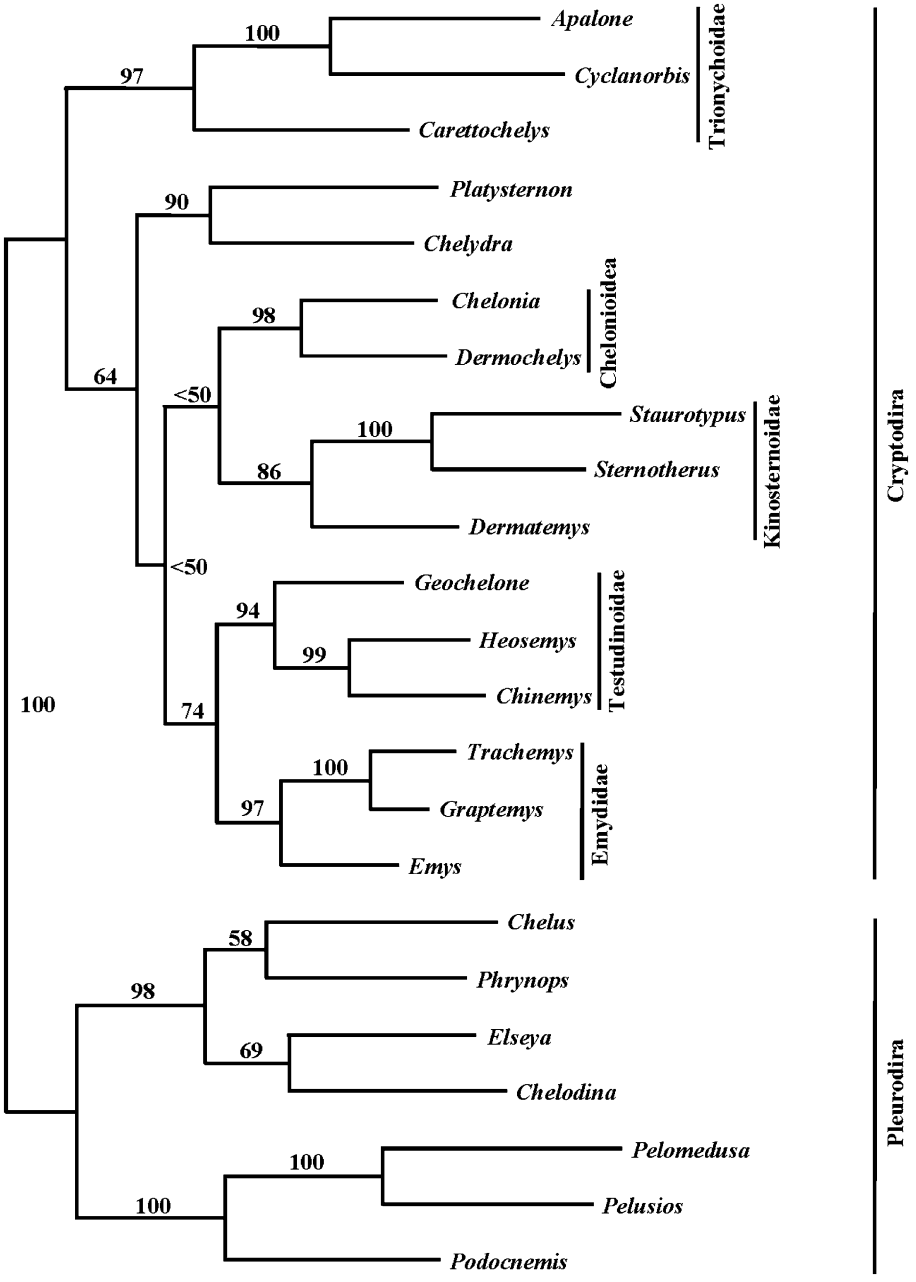

Fig. 1. Single most parsimonious tree for 23 turtles based on 892 nucleotides from cytochrome *b*, 325 nucleotides from 12S rDNA, and 115 morphological characters (Shaffer et al., 1997). Numbers near corresponding branches indicate bootstrap percentages out of 1000 bootstrap replicates. Vertical bars delineate the two turtle suborders, Cryptodira and Pleurodira, as well as several key cryptodiran taxonomic groupings referred to in the text. Tree length = 2793 steps, consistency index = 0.41, and retention index = 0.42.

conservation prioritization of turtle groups, many of which are critically imperiled (Dalton, 2003; Gibbons et al., 2000; Klemens, 2000).

Ambiguity in branching patterns among clades can be explained by two alternative hypotheses (Kraus and Miyamoto, 1991; Shaffer et al., 1997). The existing polytomies in hypotheses of turtle relationships could represent the actual history of turtle evolution or they may reflect the inability of existing data to resolve certain phylogenetic levels. In the first case, groups of turtles may have diverged so rapidly that an unresolved "hard" polytomy is a reasonably accurate representation of their evolutionary history. Alternatively, the observed lack of resolution could result from insufficient data sampling, invariant characters, or saturated molecular data. Quickly evolving mitochondrial genes can become saturated with multiple substitutions at the same position, masking evolutionary change in the observed sequence (Li, 1997). A large number of saturated characters could provide strong enough misleading signal to overturn information from a smaller set of slowly evolving characters (e.g., morphological traits), resulting in a

lack of phylogenetic resolution among deep nodes of a tree. Even so, no recent research has questioned the reality of the deepest recognized division within extant turtles between the reciprocally monophyletic Cryptodira and Pleurodira (Fujita et al., 2004; Gaffney, 1984; Shaffer et al., 1997). However, relationships among some of the major cryptodiran groups have been much more difficult to determine.

We analyzed existing mtDNA and new nuDNA sequence data to clarify fundamental phylogenetic relationships in turtles. These data have already contributed to our understanding of the tempo of turtle diversification (Near et al., 2005); here we provide a detailed analysis of their phylogenetic performance. We subjected aligned sequences for 24 species of turtles from across all extant families (Shaffer et al., 1997; Fig. 1) plus alligator (*Alligator mississippiensis*) and chicken (*Gallus gallus*) to maximum parsimony (MP), maximum likelihood (ML), and Bayesian phylogenetic analyses. To obtain nuDNA data, we sequenced and aligned >90% (2793 base pairs) of the recombination activase gene-1 (RAG-1). RAG-1 is a single-copy, intron-free, protein-coding gene roughly 3 kilobases (kb) in length that occurs throughout vertebrates (Bernstein et al., 1996; Carlson et al., 1991; Schatz et al., 1989). The utility of RAG-1 as a phylogenetic tool for resolving relatively deep relationships has been established in birds (Groth and Barrowclough, 1999), mammals (Murphy et al., 2001), squamates (Townsend et al., 2004), and sharks (G. Naylor, unpubl. data). We demonstrate that this gene is also valuable for understanding phylogenetic relationships among turtles and for revealing schisms between the models underlying the main methods used in phylogenetic analysis.

2. Materials and methods

2.1. Choice of taxa

We used all 23 extant turtle taxa included by Shaffer et al. (1997) in this study to facilitate direct comparisons between results from morphological characters, mtDNA, and nuDNA data sets (Table 1). These taxa were originally chosen because they represent all currently recognized turtle families and subfamilies (Ernst and Barbour, 1989; Gaffney and Meylan, 1988), as well as a few key lower-level exemplars, and could address several issues regarding contentious areas of turtle systematics (see Fujita et al., 2004; Shaffer et al., 1997). RAG-1 sequence from one additional taxon, *Lissemys punctata*, was also included. The sequence listed as *Lissemys punctata* by Shaffer et al. (1997) actually came from a *Cyclanorbis senegalensis* sample, based on its virtual sequence identity with that species that emerged in a phylogenetic analysis of all living trionychoid species (Engstrom et al., 2004; T. Engstrom, pers. comm.). Therefore, we included both *L. punctata* and *C. senegalensis* as two representative members of the softshell turtle subfamily Cyclanorbinae (Engstrom et al., 2004; Ernst and Barbour, 1989). The original misidentification had no misleading effects on the results presented by Shaffer et al. (1997).

Table 1
Twenty-four turtle species for which RAG-1 was sequenced and analyzed for this study

Pleurodira	
Pelomedusidae	
	Pelusios williamsi
	Pelomedusa subrufa
Podocnemidae	
	Podocnemis expansa
Chelidae	
	Chelodina longicollis
	Chelus fimbriata
	Elseya latisternum
	Phrynops gibbus
Cryptodira	
Chelydridae	
	Chelydra serpentina
	Platysternon megacephalum
Cheloniidae	
	Chelonia mydas
Dermochelyidae	
	Dermochelys coriacea
Trionychidae	
	Apalone spinifera
	Cyclanorbis senegalensis
	Lissemys punctata
Carettochelyidae	
	Carettochelys insculpta
Kinosternidae	
	Sternotherus odoratus
	Staurotypus triporcatus
Dermatemydidae	
	Dermatemys mawii
Emydidae	
	Emys marmorata
	Graptemys pseudogeographica
	Trachemys scripta
	Heosemys spinosa
	Chinemys reevesii
Testudinidae	
	Geochelone pardalis

Family designations are based on Ernst and Barbour (1989).

2.2. Data collection

We designed PCR primers based on conserved regions found in an alignment of RAG-1 sequences available on GenBank for *Gallus gallus* (M58530, Carlson et al., 1991), *Alligator mississippiensis*

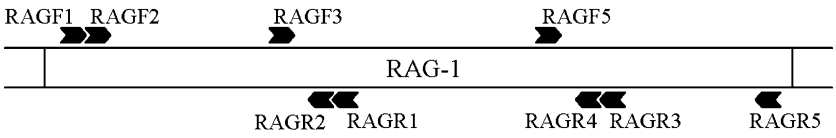

RAGF1	CCWGAWGARATTCAGCAYCC
RAGR1	GCAAGATCTCTTCATCRCATTC
RAGF2	GAGATCATTYGAAAAGGCACC
RAGR2	GATGTTCAGGAAGGATTTCACT
RAGF3	AGAACCTGCATCCTRAAGTGC
RAGR3	CTCAGGATGGCTGTCAGAGTC
RAGR4	TGCAACACAGCTCTGAATTGG
RAGF5	GAGATGTCAGYGAGAAGCATG
RAGR5	GACATCCTCCATTTCATAGC

Fig. 2. Names, positions, and sequences of oligonucleotide primers used for amplification and sequencing of RAG-1. Sequences are given in the 5′ to 3′ direction. All primers were used for both amplification and sequencing.

(AF143724, Groth and Barrowclough, 1999), and *Gavialis gangeticus* (AF143725, Groth and Barrowclough, 1999). RAG-1 was amplified and sequenced in three segments requiring a total of nine oligonucleotide primers (Fig. 2). Each segment was ~1 kb in length and overlapped with its neighboring sequence(s) at roughly 100 nucleotide bases. Also, each segment was sequenced in both directions, allowing sequence confirmation at roughly half of the nucleotide sites.

In most cases we were able to use the same individual (usually the same DNA extraction) for RAG-1 sequencing as was used for mtDNA sequencing in Shaffer et al. (1997). Some DNA samples proved too degraded for consistent RAG-1 amplification; when this occurred, new tissue for that taxon was obtained (either muscle, liver, blood, tail tips, or skin snips), and total genomic DNA was extracted using the High Pure PCR Template Preparation Kit (Roche Molecular Biochemicals) following the manufacturer's instructions. Templates were diluted with sterile, deionized water as needed for amplification of RAG-1.

We amplified RAG-1 segments in a Perkin Elmer GeneAmp PCR System 2400. PCR was conducted in 50 μL volumes with 0.5–1.0 μg of purified genomic DNA, 1× PCR buffer (10 mM Tris–HCl, 50 mM KCl, and 0.1% Triton X-100), 1.0–1.5 mM $MgCl_2$, 0.1 mM dNTPs, 0.5 μM forward and reverse primer, and 1 U *Taq* DNA polymerase (Promega). The thermocycling procedure consisted of an initial denaturation at 94 °C for 5 min, followed by 30 cycles of denaturation at 94 °C for 30 s, annealing at 55 °C for 60 s, and extension at 72 °C for 90 s. An additional extension at 72 °C for 5 min followed the last cycle. We used a touchdown thermocycling procedure for templates that were difficult to amplify. The touchdown program began with an initial denaturation at 94 °C for 5 min, followed by a phase consisting of two cycles of 94 °C denaturation for 30 s, 62 °C annealing for 60 s, and 72 °C extension for 90 s. This procedure was followed by four identical cycle phases, with a 2 °C reduction in annealing temperature for each phase (60, 58, 56, and 54 °C). The final phase consisted of 30 cycles identical to the previous cycles, but with a 52 °C annealing temperature. A final extension at 72 °C for 5 min ended the touchdown procedure.

Entire reactions were run on 1.5% low-melt TBE agarose gels in the presence of ethidium bromide. Bands were cut from gels, combined with 500 μL sterile deionized water, and melted at 90 °C for 5 min. These isolated templates were run in a second PCR, with conditions identical to the first, to generate DNA for sequencing. Products from this second PCR were concentrated and purified in Microcon M-100 microconcentrators (Amicon). PCR products were resuspended with 12 μL sterile, deionized water, and their concentration was found through fluorometry. These products were cycle sequenced in both directions using the ABI Prism BigDye Terminator Cycle Sequencing Ready Reaction Mix (PE Applied Biosystems). Reactions were run in 20 μL volumes containing ~80 ng cleaned PCR product, 0.04 M Tris–HCl (pH 9), 1 mM $MgCl_2$, 0.3 mM primer, and 4 μL Terminator Ready Reaction Mix. The thermocycling procedure consisted of 45 cycles of 96 °C for 30 s, 50 °C for 30 s, and 60 °C for 4 min. Sequenced products were precipitated with isopropanol, dried following manufacturer's instructions, and sequenced at the Iowa State University DNA Sequencing and Synthesis Facility on an ABI 377 automated sequencer. RAG-1 sequences were deposited in the GenBank database under Accession Nos. AY687901–AY687924.

2.3. Data analysis

Complete sequences for each taxon were assembled with Sequence Navigator vers. 1.0.1 (Applied Biosystems 1994) and aligned using Sequence Alignment Program (Se-Al) vers. 1.d1 (Rambaut, 1995). Partition homogeneity tests were calculated using PAUP* 4.0b3a (Swofford, 2001) with 1000 replicates to test the combinability of (1) RAG-1 vs. mtDNA, (2) RAG-1 vs. morphological data, and (3) RAG-1 vs. mtDNA + morphological data.

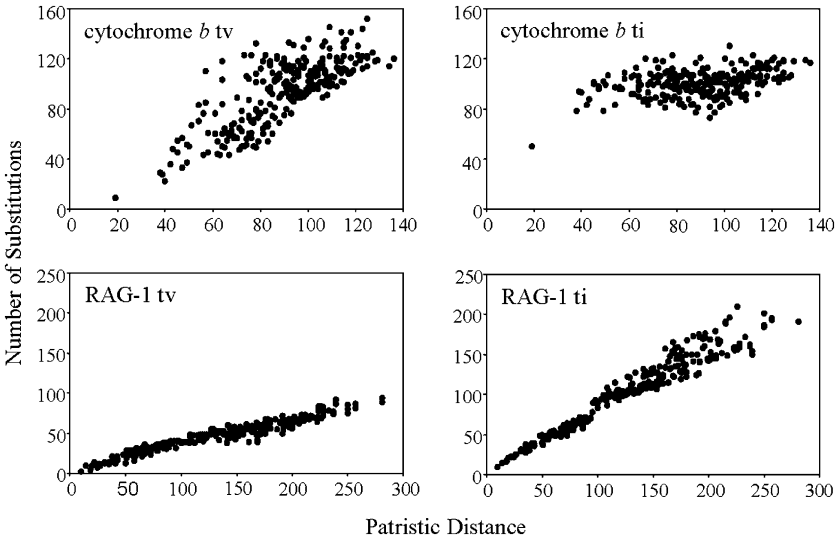

Fig. 3. The absolute number of transition (ti) and transversion (tv) substitutions plotted against patristic distance for cytochrome *b* and RAG-1. Points represent pairwise comparisons among all 23 turtle species used.

We performed both maximum parsimony (MP) and maximum likelihood (ML) analyses using PAUP*; Bayesian analyses were performed with MrBayes (v3.0B4) (Huelsenbeck and Ronquist, 2001). Rather than make any assumptions about the monophyly of any turtle clades (Fujita et al., 2004; Gaffney, 1975; Gaffney and Meylan, 1988; Gaffney et al., 1991; Shaffer et al., 1997), we instead designated *Alligator* and *Gallus* as the outgroup. The inclusion of several additional non-chelonian outgroup taxa was explored, including *Gavialis*, *Mus*, *Xenopus*, and *Onchorhynchus*; their inclusion did not substantively alter the results, and their exclusion allowed greater confidence in alignments as well as greatly increased computational efficiency. We included all RAG-1 sequence data because we detected little base composition deviancy and no saturation (see below; Fig. 3).

In MP analyses, heuristic searches were performed with 10 replicates of random taxon addition, accelerated character transformation (ACCTRAN) optimization, tree bisection-reconnection (TBR) branch swapping, zero-length branches collapsed to yield polytomies, and gaps coded as missing data. As an indication of the robustness of clades, we used bootstrapping (Felsenstein, 1985) with 1000 replicates. We regard bootstrap values $\geqslant 90\%$ indicative of strong support for a clade, while values >70 and <90% indicate moderate support, and values <70% indicate weak support (sensu Shaffer et al., 1997).

We performed ML analysis of RAG-1 using the TrN + I + Γ model of DNA sequence evolution, as determined by both the Likelihood Ratio Test and Akaike Information Criterion in Modeltest 3.06 (Posada and Crandall, 1998). The TrN model (Tamura and Nei, 1993) allows for unequal base frequencies, one class for transversions, and two classes for transitions; we also accounted for the proportion of invariable sites (I) and among-site rate variation (Γ). Modeltest found the GTR + I + Γ model most appropriate for analysis of the combined RAG-1/mtDNA data set. The GTR model (Rodriguez et al., 1990) allows for unequal base frequencies, four classes for transversions, and two classes for transitions. For both the TrN + I + Γ and GTR + I + Γ models, empirical base frequencies were used whereas the rates for transitions and transversions, the proportion of invariable sites (I), and the Γ-shape parameter (α) were estimated by PAUP*. Again, 1000 bootstrap replicates were used as an indication of support for clades.

Bayesian analyses were run under the GTR + I + Γ model of nucleotide substitution, the parameters of which were estimated by MrBayes. Analyses were initiated with random starting trees and run for 2.0×10^6 generations; the Markov chains were sampled every 1000 generations. Log-likelihood scores of sample points were plotted against generation to determine when the Markov chain reached stationarity (i.e., the "burn-in" time), and sample points prior to "burn-in" were discarded. Three independent analyses were performed and checked for consistency. Trees from sample points following the burn-in were combined into a 50% majority rule consensus tree; the percentage of samples recovering a given clade reflects the clade's posterior probability. Posterior probabilities $\geqslant 95\%$ are regarded as strong support for a given clade.

3. Results

3.1. RAG-1 relative to cytochrome b

Throughout the section, we compare RAG-1 characteristics to the characteristics of the cytochrome *b* data of Shaffer et al. (1997). In that study, cytochrome *b* contributed the greatest overall number of characters (cytochrome *b*: 894, 12S rDNA: 245, and morphology:

115) to the mtDNA/morphology combined analysis, as well as the overwhelming majority of parsimony-informative characters (cytochrome *b*: 413, 12S rDNA: 72, and morphology: 93). The protein-coding nature of cytochrome *b* in turn allows for more direct comparisons with RAG-1, such as characteristics at various codon positions. Although the same taxa have also been sampled for R35 (Fujita et al., 2004; Near et al., 2005), we did not make direct comparisons with this non-coding nuclear intron.

3.2. Sequence variation, base composition, and saturation analysis

Most of the 3 kb of RAG-1 was sequenced and aligned for all 24 turtle species included in this study, resulting in a sequence alignment 2793 nucleotide bases in length. Overall, a high level of similarity was observed, making sequence alignment straightforward and unambiguous. We discovered no introns, and indels were infrequent and always occurred in multiples of three, thus not interrupting the reading frame of the gene. *Trachemys* and *Graptemys* shared an apparent nine base pair deletion, while a three base pair deletion was found in *Carettochelys* and a three base pair insertion was detected in *Podocnemis*.

Variation in RAG-1 occurred at 727 (26.0%) sites, 436 of which were parsimony-informative. Within codons, 147 variable sites occurred at first positions (90 parsimony-informative), 91 at second positions (44 parsimony-informative), and 489 at third positions (302 parsimony-informative). Uncorrected *p*-distances (Table 2) between taxa ranged from 0.4% (*Graptemys* vs. *Trachemys*) to 10.2% (*Podocnemis* vs. *Lissemys*). These results compare to 57.8% sites variable in cytochrome *b* (148 variable sites at first positions, 81 at second positions, and 288 at third positions), and *p*-distances ranging from 6.6 to 30.3%. The much greater level of variability in cytochrome *b*, coupled with a shorter sequence length, produced a comparable number of parsimony-informative sites (413 from cytochrome *b*) to that from RAG-1. As with other RAG-1 data sets (e.g., Groth and Barrowclough, 1999), the first ~1 kb was somewhat more variable than the final ~2 kb: 31.4% sites were variable in the first 1000 bases versus 23.0% sites variable in the final 1793 bases.

RAG-1 nucleotide base composition shows a slight bias toward adenine, whereas the remaining three bases are present at similar frequencies (30.7% adenine, 21.5% cytosine, 24.1% guanine, and 23.8% thymine). This remarkable base composition homogeneity holds across taxa when all positions are considered ($\chi^2 = 8.34$, df = 69, $p = 1.00$) and even when the highly variable third positions are tested alone ($\chi^2 = 13.40$, df = 69, $p = 1.00$). Cytochrome *b* sequences have a higher degree of bias in base composition with high levels of adenine and cytosine and very low levels of guanine (30.2% adenine, 30.6% cytosine, 12.1% guanine, and 27.1% thymine) as is typical of mtDNA. Cytochrome *b* base composition is homogeneous across the taxa when all codon positions are considered simultaneously ($\chi^2 = 49.03$, df = 66, $p = 0.94$); however, the highly variable third positions of cytochrome *b* display significant heterogeneity in base composition among taxa ($\chi^2 = 149.65$, df = 66, $p \ll 0.0001$).

To assess the degree of saturation in the cytochrome *b* and RAG-1 data sets, we plotted the observed numbers of transversions and transitions against patristic distance (inferred steps along the tree) for all pairwise comparisons of taxa (Fig. 3). Saturation is evident if this relationship asymptotes as patristic distance increases, indicating that inferred multiple substitutions are occurring. There is no indication of saturation in RAG-1 transitions or transversions, indicating that both data partitions may be informative across the breadth of turtle phylogeny; a similar result was found for the nuclear intron R35 for many of these taxa (Fujita et al., 2004). Cytochrome *b* transversions may show a mild pattern of saturation, although the effect is relatively slight. In contrast, the pattern observed in cytochrome *b* transitions is nearly horizontal, indicating a high level of saturation at these sites. We also looked for saturation at various codon positions in RAG-1; no saturation was evident at any position (results not shown).

3.3. Phylogenetic analyses

Partition homogeneity tests demonstrated that some aspects of the separate data sets were combinable for subsequent phylogenetic analysis and others were not. RAG-1 data were marginally combinable with mtDNA data ($p = 0.08$), but not with morphological data ($p = 0.002$) or with the combined mtDNA and morphology data set ($p = 0.001$). We therefore conducted both separate and combined molecular analyses.

Unweighted MP analysis of RAG-1 (Fig. 4A) revealed two most parsimonious trees 1812 steps in length. These trees differed only on their placement of *Chelydra*. One tree placed *Chelydra* as the sister-group to the Chelonioidea (a group containing the families Cheloniidae and Dermochelyidae and represented here by *Chelonia* and *Dermochelys*), whereas the second tree placed *Chelydra* as the sister group to the Kinosternoidae (a group containing the families Kinosternidae and Dermatemydidae and represented here by *Staurotypus*, *Sternotherus*, and *Dermatemys*). When we bootstrapped the data set under parsimony, both of the alternative branches in question received <50% BP, leaving the relationships ambiguous. In this analysis, the "Trionychoidae" (a generally recognized clade containing the families Trionychidae [*Apalone*, *Cyclanorbis*, and *Lissemys*] and Carettochelyidae [*Carettochelys*]) is paraphyletic with respect to all remaining turtles, although its monophyly is not statistically rejected.

Table 2
Genetic distances among turtles species used in this study

	1	2	3	4	5	6	7	8	9	10	11	12	13	14	15	16	17	18	19	20	21	22	23	24
1. *Apalone*	—	—	0.203	0.231	0.236	0.226	0.212	0.203	0.235	0.231	0.217	0.203	0.215	0.216	0.212	0.211	0.202	0.233	0.221	0.222	0.243	0.240	0.284	0.231
2. *Lissemys*	0.052	—	—	—	—	—	—	—	—	—	—	—	—	—	—	—	—	—	—	—	—	—	—	—
3. *Cyclanorbis*	0.049	0.011	—	0.234	0.249	0.246	0.223	0.224	0.243	0.230	0.249	0.232	0.241	0.243	0.233	0.224	0.225	0.234	0.242	0.234	0.263	0.279	0.303	0.251
4. *Carettochelys*	0.076	0.093	0.093	—	0.221	0.233	0.196	0.206	0.230	0.219	0.228	0.201	0.213	0.228	0.213	0.205	0.213	0.241	0.234	0.234	0.257	0.271	0.293	0.246
5. *Platysternon*	0.058	0.075	0.074	0.076	—	0.201	0.174	0.195	0.215	0.185	0.204	0.175	0.185	0.187	0.193	0.180	0.186	0.257	0.229	0.218	0.241	0.274	0.282	0.267
6. *Chelydra*	0.058	0.076	0.076	0.075	0.023	—	0.174	0.174	0.220	0.189	0.214	0.185	0.167	0.188	0.178	0.180	0.181	0.222	0.215	0.212	0.245	0.263	0.267	0.246
7. *Chelonia*	0.062	0.081	0.080	0.080	0.030	0.025	—	0.133	0.200	0.166	0.197	0.158	0.168	0.166	0.167	0.151	0.147	0.215	0.188	0.205	0.230	0.225	0.250	0.240
8. *Dermochelys*	0.065	0.079	0.079	0.082	0.029	0.025	0.019	—	0.197	0.179	0.183	0.164	0.166	0.168	0.169	0.158	0.163	0.221	0.186	0.195	0.226	0.235	0.270	0.214
9. *Staurotypus*	0.067	0.086	0.084	0.086	0.035	0.031	0.038	0.037	—	0.200	0.164	0.197	0.215	0.203	0.202	0.191	0.207	0.238	0.231	0.234	0.248	0.249	0.262	0.251
10. *Dermatemys*	0.067	0.085	0.083	0.084	0.035	0.030	0.037	0.038	0.034	—	0.197	0.168	0.187	0.198	0.183	0.173	0.183	0.219	0.207	0.206	0.232	0.254	0.265	0.241
11. *Sternotherus*	0.063	0.082	0.081	0.081	0.029	0.026	0.033	0.032	0.013	0.026	—	0.180	0.209	0.206	0.195	0.194	0.192	0.241	0.220	0.223	0.240	0.251	0.246	0.238
12. *Geochelone*	0.066	0.081	0.080	0.081	0.027	0.033	0.037	0.038	0.045	0.043	0.039	—	0.145	0.156	0.167	0.145	0.152	0.225	0.211	0.205	0.229	0.258	0.254	0.231
13. *Heosemys*	0.061	0.076	0.076	0.074	0.021	0.028	0.033	0.034	0.040	0.038	0.034	0.018	—	0.129	0.175	0.152	0.157	0.243	0.217	0.217	0.243	0.258	0.261	0.240
14. *Chinemys*	0.060	0.076	0.076	0.075	0.019	0.025	0.030	0.032	0.038	0.036	0.032	0.016	0.009	—	0.166	0.163	0.173	0.249	0.226	0.209	0.244	0.258	0.266	0.240
15. *Trachemys*	0.057	0.073	0.072	0.070	0.015	0.021	0.027	0.026	0.033	0.031	0.026	0.025	0.019	0.017	—	0.066	0.137	0.226	0.206	0.217	0.241	0.263	0.266	0.241
16. *Graptemys*	0.056	0.073	0.072	0.069	0.016	0.022	0.028	0.027	0.033	0.032	0.027	0.025	0.020	0.018	0.004	—	0.120	0.215	0.197	0.224	0.234	0.250	0.252	0.230
17. *Emys*	0.054	0.071	0.070	0.070	0.013	0.019	0.025	0.026	0.032	0.032	0.026	0.023	0.018	0.015	0.008	0.008	—	0.231	0.212	0.217	0.238	0.251	0.259	0.233
18. *Chelus*	0.071	0.086	0.085	0.085	0.054	0.054	0.059	0.056	0.063	0.062	0.057	0.058	0.053	0.052	0.052	0.052	0.051	—	0.193	0.210	0.211	0.262	0.262	0.240
19. *Phrynops*	0.070	0.085	0.085	0.085	0.052	0.054	0.057	0.055	0.062	0.059	0.056	0.057	0.052	0.051	0.050	0.051	0.049	0.013	—	0.188	0.217	0.247	0.241	0.221
20. *Elseya*	0.070	0.086	0.086	0.085	0.051	0.053	0.056	0.055	0.062	0.060	0.057	0.058	0.054	0.052	0.051	0.051	0.049	0.026	0.026	—	0.189	0.266	0.273	0.241
21. *Chelodina*	0.071	0.087	0.086	0.087	0.057	0.056	0.061	0.060	0.067	0.065	0.061	0.061	0.057	0.056	0.054	0.054	0.053	0.030	0.030	0.027	—	0.285	0.291	0.269
22. *Pelomedusa*	0.080	0.097	0.096	0.095	0.061	0.064	0.066	0.065	0.069	0.069	0.066	0.069	0.066	0.063	0.060	0.060	0.061	0.048	0.047	0.046	0.052	—	0.195	0.247
23. *Pelusios*	0.084	0.100	0.099	0.100	0.062	0.065	0.068	0.067	0.070	0.070	0.067	0.070	0.066	0.063	0.062	0.063	0.061	0.049	0.048	0.048	0.053	0.010	—	0.241
24. *Podocnemis*	0.090	0.102	0.100	0.099	0.075	0.075	0.078	0.077	0.083	0.085	0.080	0.079	0.076	0.075	0.072	0.072	0.072	0.063	0.063	0.059	0.062	0.054	0.056	—

RAG-1 *p*-distances are below diagonal; cytochrome *b* *p*-distances are above diagonal.

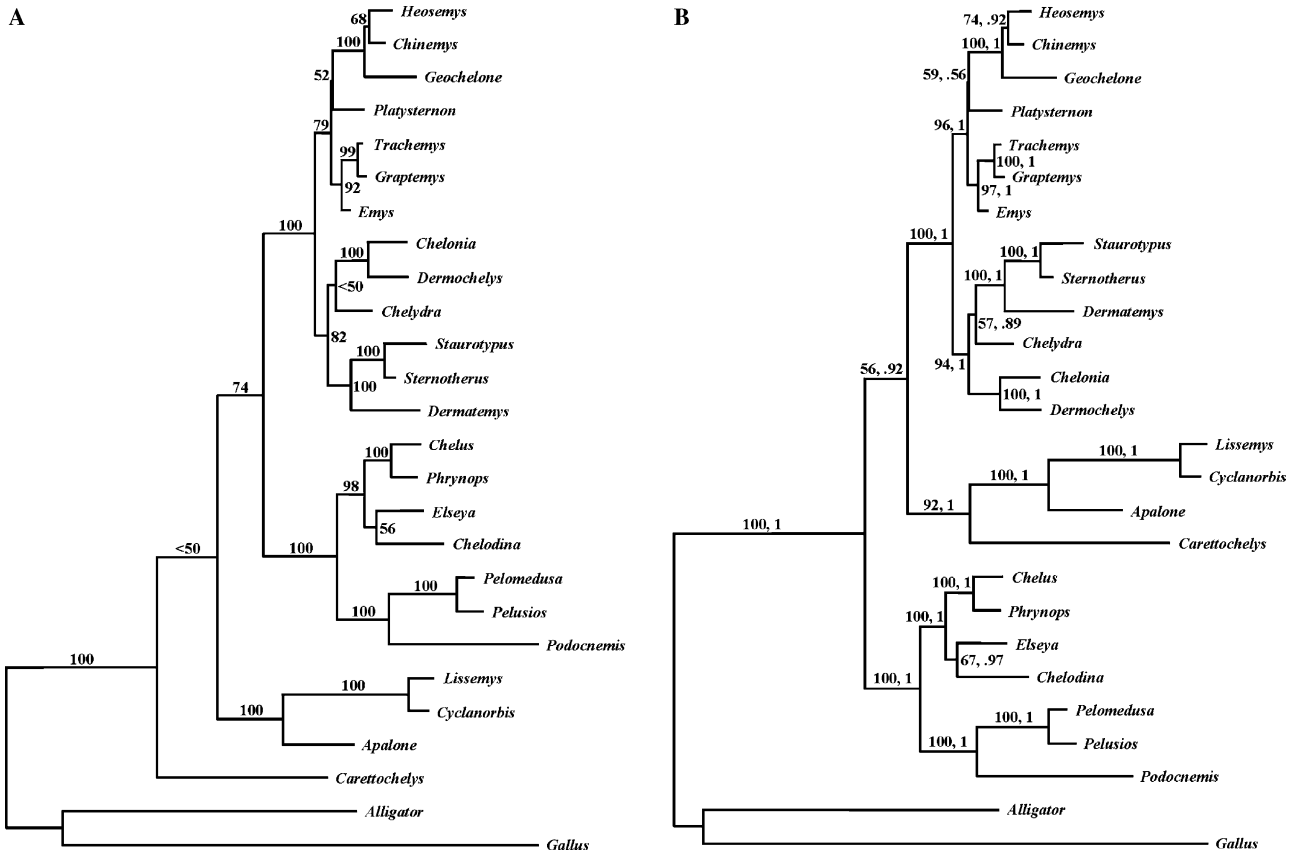

Fig. 4. (A) Maximum parsimony phylogram for 2793 nucleotides of RAG-1 for 24 turtle species. Numbers near corresponding branches indicate percentages out of 1000 bootstrap replicates. One of two most parsimonious trees is depicted; the alternate tree placed *Chelydra* as the sister-group to the dermatemydids with weak statistical support. Tree length = 1812 steps, consistency index = 0.68, retention index = 0.68. (B) Maximum likelihood and Bayesian analysis phylogram of RAG-1. Numbers near corresponding branches indicate percentages out of 1000 bootstrap replicates for ML followed by posterior probabilities for Bayesian analysis. ML was run using the TrN + I + Γ model of DNA sequence evolution. Parameters for the model were estimated by PAUP*; base frequencies: A = 0.321, C = 0.212, G = 0.224, and T = 0.244; transversion and transition rates: all transversions = 1, A–G transitions = 4.364, and C–T transitions = 6.032; I = 0.408; α (Γ shape parameter) = 1.310. Bayesian analysis was run under the GTR + I + Γ model. Mean values of parameters for the GTR + I + Γ model of nucleotide substitution were estimated by MrBayes; base frequencies: A = 0.320, C = 0.208, G = 0.225, and T = 0.247; transversion and transition rates: G–T transversions = 1, C–G transversions = 1.192, A–T transversions = 0.984, A–C transversions = 1.288, A–G transitions = 4.929, and C–T transitions = 6.856; I = 0.395; α (Γ shape parameter) = 1.466.

The topology found under ML analysis of RAG-1 was identical to that found in Bayesian analysis (Fig. 4B). This topology differed from the MP tree in two respects. First, the Trionychoidae is monophyletic and the sister group to the other cryptodires (sensu Shaffer et al., 1997) rather than paraphyletic with respect to all other turtles (cf. Figs. 4A and B). Second, ML and Bayesian analysis placed *Chelydra* as the sister group to the Kinosternoidae rather than to the Chelonioidea, though with low statistical support. In other respects, tree topology and statistical support found under ML and Bayesian analysis are concordant with those found under MP. Branches linking *Platysternon* to the Testudinoidae (a group containing the families Testudinidae [*Geochelone*] and Geoemydidae [*Heosemys*, *Chinemys*]) and *Chelydra* to the Kinosternoidae are very short, in agreement with the low level of statistical support for these branches in MP analyses.

The tree topologies found using the nuDNA sequences (Fig. 4) are identical to those based on the combined analysis of morphology and mtDNA sequences (Shaffer et al., 1997; Fig. 1) in all respects except (1) the Chelydridae (*Chelydra*) and Platysternidae (*Platysternon*) are not sister taxa, contrary to results of morphological analyses and (2) the Trionychoidae again forms a paraphyletic group that is the sister taxon to all other extant turtles in our MP analysis, rendering the Cryptodira non-monophyletic. However, ML and Bayesian analyses recover the traditional placement of the Trionychoidae with weak statistical support (56% BP under ML and .92 posterior probability under Bayesian analysis). Moreover, under ML and Bayesian analyses, deep Cryptodiran branches achieved a level of support markedly greater than that attained from the morphology/mtDNA data (Fig. 4B).

In the morphology/mtDNA-based tree (Fig. 1), *Platysternon* and *Chelydra* group as sister taxa with 90% bootstrap support. This relationship was not found individually for cytochrome *b* or 12S, but was strongly supported (94% BP) by the morphological data, leading to the result obtained in the combined analysis (Shaffer et al., 1997). In contrast, deeper branches with strong statistical support separate these two taxa in the RAG-1 trees (Fig. 4). Morphology/mtDNA also placed *Platysternon* and *Chelydra* as the sister group to all non-trionychoid cryptodires, although with low support (64% BP). RAG-1 places neither *Chelydra* nor *Platysternon* in the position indicated by morphology/mtDNA; rather, *Chelydra* appears as the sister group to the Chelonioidea or the Kinosternoidae, whereas *Platysternon* resides with the Testudinoidae. However, within each of those clades, the branches leading to *Chelydra* and *Platysternon* received low support, making their exact relationships within their new respective groupings unclear; when taxon sampling for the R35 intron is combined with the RAG-1 and cytochrome *b* data, these relationships receive additional statistical support (Near et al., 2005).

A Templeton Test (Larson, 1994; Templeton, 1983) was conducted under MP to determine if (1) the RAG-1 data were in significant disagreement with the morphology/mtDNA topology of Shaffer et al. (1997) or (2) the RAG-1 data were inconsistent with *Chelydra*/*Platysternon* monophyly. When the RAG-1 data (with the exclusion of *Lissemys* and the outgroup taxa *Alligator* and *Gallus*, which were not part of the morphology/mtDNA data set) were constrained to fit the morphology/mtDNA topology, the tree (1185 steps) was significantly longer ($p = 0.0004$) than the best tree found with RAG-1 (1169 steps). To test for signal of *Chelydra*/*Platysternon* monophyly, hypothetical trees were constructed for every possible placement of a monophyletic *Chelydra* + *Platysternon*, given that the topologies of the RAG-1 and morphology/mtDNA trees were identical in all other respects. The shortest tree found when constraining RAG-1 to group *Chelydra* and *Platysternon* together was 1183 steps in length, which again is significantly longer ($p = 0.0043$) than the best RAG-1 tree. These results indicate that RAG-1 is inconsistent with a monophyletic (*Chelydra* + *Platysternon*), regardless of its placement on the tree. However, when we performed a Shimodaira–Hasegawa test (Shimodaira and Hasegawa, 1999) under ML, the topology found by Shaffer et al. (1997) could not be rejected ($p = 0.109$), nor could eight other hypothetical trees demonstrating *Chelydra* + *Platysternon* monophyly ($p = 0.058$–0.176).

The results for RAG-1 and mtDNA sequences were combined into one data set containing 873 parsimony-informative characters. The results of this combined analysis under MP (Fig. 5A) and ML or Bayesian algorithms (Fig. 5B) are virtually identical to the respective analyses for RAG-1 alone. This combined MP analysis is identical in topology to the MP RAG-1 tree (Fig. 4A), except that *Platysternon* moved from its position as the sister taxon to the Testudinoidae to being the sister taxon to a clade comprising the Testudinoidae and the family Emydidae. The topology found under ML analysis of the combined data set is identical to that found with Bayesian analysis (Fig. 5B), and both supported the placement of *Chelydra* with the Chelonioidea. Also, ML and Bayesian analysis recovered a monophyletic Cryptodira, placing the Trionychoidae as the sister group to the rest of the cryptodires, although with low statistical support—61% BP under ML and .90 posterior probability in Bayesian analysis.

Our most unexpected finding concerns the phylogenetic placement of the Trionychoidae, which shows the greatest degree of lability between MP, ML, and Bayesian analyses. MP analyses of RAG-1 alone or of the total RAG-1 plus mtDNA dataset place the Trionychoidae as a paraphyletic group with respect to all remaining turtles, although with relatively weak support (Figs. 4A and 5A). In contrast, ML and Bayesian analyses place this group in a more traditional position as the sister taxon to the rest of the Cryptodira (sensu Shaffer et al., 1997); this placement also has low support (Figs. 4B and 5B). Templeton tests using the parsimony criterion show that the RAG-1 data alone or combined with the mitochondrial DNA data do not reject the traditional phylogenetic placement of the Trionychoidae ($p = 0.739$ and $p = 0.210$, respectively). The traditional placement was the best fit under the Shimodaira–Hasegawa test, but here the basal position was also not significantly different ($p = 0.606$ and $p = 0.680$, respectively). These results imply that the long-held view of the monophyly of the Cryptodira is questionable.

4. Discussion

We sequenced nearly all of the 3 kb nuclear RAG-1 gene for turtles representing all currently recognized turtle families to resolve ambiguous areas of their evolutionary relationships. RAG-1 sequences are quite "clean" compared to cytochrome *b* sequences from the same animals; RAG-1 is not saturated, has relatively low base composition bias, and has a very homogeneous base composition across the included taxa. The molecular characteristics of RAG-1 across turtles imply that this remarkable gene contains nearly ideal properties for phylogenetic analysis; for turtles, its performance is similar to the R35 nuclear intron (Fujita et al., 2004). Indeed, the relatively large, slowly evolving RAG-1 data set confirmed most of the uncertain relationships among major turtle groups suggested by morphology/mtDNA and nuDNA, and clarified a case of apparent morphological parallelism between chelydrid (*Chelydra*) and platysternid (*Platysternon*) turtles. Moreover, this data set revealed fundamental conflicts among the major methods of phylogenetic analysis that alternatively disputed (MP) and confirmed (ML and Bayesian) the

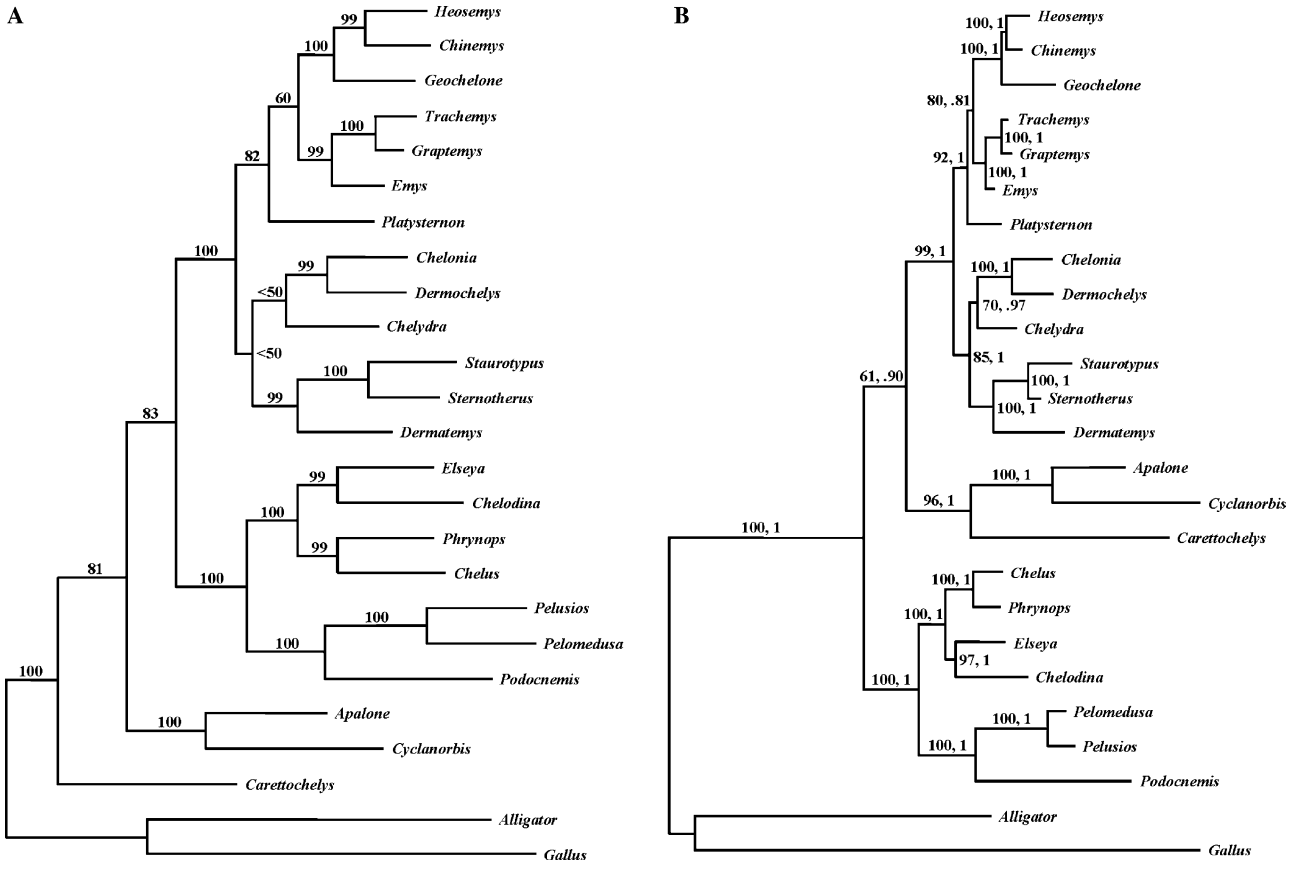

Fig. 5. (A) Maximum parsimony phylogram based on combined analysis of 2793 nucleotides from RAG-1, 892 nucleotides from cytochrome *b*, and 325 nucleotides from 12S rDNA. Numbers near corresponding branches indicate percentages out of 1000 bootstrap replicates. One of two most parsimonious trees is depicted; the alternate tree placed *Chelydra* as the sister-group to the dermatemydids with weak statistical support. Tree length = 4937 steps, consistency index = 0.49, retention index = 0.45. (B) Maximum likelihood and Bayesian analysis phylogram based on combined analysis of 2793 nucleotides from RAG-1, 892 nucleotides from cytochrome *b*, and 325 nucleotides from 12S rDNA using the GTR + I + Γ model of DNA sequence evolution. Numbers near corresponding branches indicate percentages out of 1000 bootstrap replicates for ML followed by posterior probabilities for Bayesian analysis. For ML, parameters for the model were estimated by PAUP*; base frequencies: A = 0.311, C = 0.264, G = 0.208, and T = 0.217; transversion and transition rates: G–T transversions = 1, G–C transversions = 0.632, A–T transversions = 2.316, A–C transversions = 2.595, A–G transitions = 4.082, and C–T transitions = 13.960; I = 0.315; α (Γ shape parameter) = 0.445. For Bayesian analysis, model parameters were estimated by MrBayes; base frequencies: A = 0.311, C = 0.264, G = 0.208, and T = 0.216; transversion and transition rates: G–T transversions = 1, G–C transversions = 0.651, A–T transversions = 2.414, A–C transversions = 2.666, A–G transitions = 4.178, and C–T transitions = 14.676; I = 0.310; α (Γ shape parameter) = 0.441.

monophyly of the Cryptodira, which has not been seriously questioned in nearly 200 years (Gaffney, 1984).

4.1. The case against (*Chelydra, Platysternon*)

Parallel morphological evolution appears to have misled many researchers about the phylogenetic positions of the Chelydridae and the Platysternidae. Morphological data imply a robust (94% BP) sister-group relationship between these two families, yet analyses of cytochrome *b* and 12S did not support this relationship (Shaffer et al., 1997). More convincingly, phylogenetic analyses of nuDNA data separate the two taxa by deep branches with strong statistical support: *Platysternon* groups with the Emydidae and the Testudinoidae, whereas *Chelydra* resides with the Chelonioidea and the Kinosternoidae (Fig. 4, see also Near et al., 2005). Templeton Tests (Templeton, 1983; Larson, 1994) under MP indicate that the RAG-1 sequences held no significant signal that would place *Chelydra* and *Platysternon* together anywhere in the tree, although Shimodaira–Hasegawa tests (Shimodaira and Hasegawa, 1999) under ML could not reject eight hypothetical trees containing *Chelydra* + *Platysternon* monophyly.

The placement of *Platysternon* near the testudinoids, as identified by the nuDNA data, is similar to a classical view of turtle phylogeny (Williams, 1950). Several independent lines of evidence derived from morphology, karyology, and protein electrophoresis further support this position. Morphological features indicating a close relationship between *Platysternon* and *Chelydra* have recently been regarded as either primitive to the extant cryptodires or due to parallelism (Danilov, 1998). Additionally, *Platysternon* has two biconvex cervical vertebrae, a trait

regarded as derived (Whetstone, 1978) and which is shared by testudinoids and emydids. Systematic evaluation of karyotype characteristics also supports this placement—only one event is required to explain the difference in chromosome number and pattern between *Platysternon* and testudinoid karyologies, while several chromosomal events would be needed to explain a closer relationship of *Platysternon* to the Chelydridae (Haiduk and Bickham, 1982). Furthermore, serum electrophoresis indicates that *Platysternon* is more similar to emydids and testudinoids than it is to *Chelydra* and kinosternids (Frair, 1972). Finally, a Bayesian analysis of the combined DNA sequence data from cytochrome *b*, RAG-1, and the nuclear intron R35 strongly supports the deep separation of *Platysternon* and *Chelydra* (Near et al., 2005). This collective evidence endorses the notion that *Platysternon* should not be included as a member of the Chelydridae (contra Gaffney and Meylan, 1988; Gaffney et al., 1991; Shaffer et al., 1997). Our RAG-1 results indicate that the morphological similarity between *Chelydra* and *Platysternon* likely derives from parallel adaptive evolution, a scenario found in molecular phylogenetic studies of other major groups of animals (e.g., Madsen et al., 2001) that has strong theoretical support (Orr, 2005).

The RAG-1 DNA sequence data furnish strong evidence that *Chelydra* and *Platysternon* are not sister taxa, but their exact placement within their "new" groups remains vague. The MP branch supporting a sister-group relationship between *Platysternon* and the Testudinoidae has 52% bootstrap support; the level of bootstrap support in the ML analysis is not much stronger. Maximum parsimony analysis of the morphological characters of Shaffer et al. (1997), but including only *Platysternon*, the Testudinidae, and the Emydidae, suggests that *Platysternon* is the sister taxon to the rest of this group (result not shown), as do karyological analyses (Haiduk and Bickham, 1982). This latter arrangement is supported, albeit relatively weakly, by the combined analysis of RAG-1 and mtDNA using MP, ML, and Bayesian algorithms (Fig. 5). The addition of R35 sequence data greatly strengthens this result, with very strong (posterior probability $\geqslant 95\%$) support under Bayesian analysis, and moderate (BP = 74%) support under MP (Near et al., 2005, and unpublished results).

MP, ML, and Bayesian analyses of RAG-1 differ on the exact placement of *Chelydra*: MP suggests a sister-group relationship with the Chelonioidea, whereas ML and Bayesian analysis suggests a sister-group relationship with the Kinosternoidae. Maximum parsimony analysis of the morphological characters from Shaffer et al. (1997), this time including only *Chelydra*, the Chelonioidea, and the Kinosternoidae, supports a sister-group relationship between *Chelydra* and the Chelonioidea (result not shown). This arrangement is confirmed, albeit weakly, by MP and ML analyses of the combined RAG-1 and mtDNA data sets, and quite strongly with Bayesian analysis (Fig. 5), although the addition of the R35 intron does not support this conclusion (Near et al., 2005).

Clearly, the available molecular data do not provide convincing evidence for the exact arrangement of *Chelydra*. The inability of RAG-1 to position this taxon lies in the fact that there are too few informative characters to render a strongly supported placement, rather than many homoplastic characters contributing noise and thus disrupting a clean signal. This finding suggests that the addition of *Macrochelys temminckii*, the only other living chelydrid (Ernst and Barbour, 1989), may help resolve this problem.

4.2. Turtle phylogeny

RAG-1 generally lends great stability to, and confidence in, the overall knowledge of turtle phylogeny (Fig. 4B). Most of the phylogenetic hypotheses tested by Shaffer et al. (1997) and Fujita et al. (2004) are strengthened by analysis of RAG-1: the Old World pond turtles (represented by *Chinemys* and *Heosemys*) form a monophyletic group and are not paraphyletic with respect to the tortoises; *Staurotypus* is included in the Kinosternoidae (not closer to the Testudinoidea), and both Australian and South American members of the Chelidae form monophyletic groups. Moreover, two major clades, the Chelidae (represented by *Chelus* and *Phrynops*) and the Pelomedusoides (represented by *Pelomedusa*, *Pelusios*, and *Podocnemis*), are again supported in the Pleurodira.

Until recent assessment of mtDNA data (Shaffer et al., 1997), the Trionychoidae was widely held to be nestled well within the Cryptodira based on various morphological characters (Gaffney and Meylan, 1988; Gaffney et al., 1991). Moreover, the Trionychoidae was regarded as the sister group of the Kinosternoidae and jointly recognized taxonomically as the Trionychoidea (Gaffney and Meylan, 1988). Regardless of analytical method, our findings deriving from re-examination of existing mtDNA sequences and morphological characters (Fig. 1), assessment of the RAG-1 data (Fig. 4), and evaluation of the combined mtDNA and nuDNA datasets (Fig. 5) are consistent with Shaffer et al. (1997), Fujita et al. (2004), and Near et al. (2005) in rendering untenable the phylogenetic hypothesis of Trionychoidea. Instead, these analyses identify the Trionychoidae as a highly divergent group with an early date of origin. This finding agrees with the substantial amount of mtDNA evolution (relative to other turtles) detected in the trionychid genus *Apalone* (Weisrock and Janzen, 2000). Furthermore, the phylogenetic position of the Trionychoidae suggested by DNA sequences corresponds to findings derived from albumin cross-reactivity (Chen et al., 1980), serology (Frair, 1983), and karyology (Bickham and Carr, 1983)—the Trionychoidae has a strikingly divergent complement of chromosomes ($2n = 66$–68 vs. $2n = 50$–56 for most other cryptodires).

Although all of the molecular data and methods of analysis concur that the Trionychoidae branches off early in the tree, they disagree fundamentally on its exact phylogenetic position. Maximum likelihood and Bayesian examination of RAG-1 alone or combined with mtDNA data (Figs. 4B and 5B) weakly place Trionychoidae as the sister taxon to a clade comprising all other cryptodirans. In contrast, MP analyses of RAG-1 alone and combined with mtDNA data provide moderate support that the Cryptodira is not monophyletic and that the "Trionychoidae" encompasses the first two splits among all extant turtles (Figs. 4A and 5A), a finding that diverges from the prevailing views of turtle systematics over the past 200 years (Dumeril, 1806; Dumeril and Bibron, 1835; Gaffney, 1984; Gaffney and Meylan, 1988; Gaffney et al., 1991; Shaffer et al., 1997). If true, these latter two MP phylogenetic analyses suggest that non-trionychoid cryptodiran turtles may actually retain a number of plesiomorphic morphological traits that do not provide evidence of Cryptodira monophyly.

The molecular work therefore implies significant value in revisiting the morphological and paleontological evidence (e.g., for a similar approach involving elasmobranchs, see Maisey et al., 2004). Examining Appendix 4 of Shaffer et al. (1997) reveals 21 morphological characters that distinguish the Cryptodira from the Pleurodira (characters 6–9, 12–14, 16, 17, 20–23, 25, 26, 32, 34, 39, and 107–109); in 11 of these cases (characters 6–9, 12, 13, 16, 25, 34, 107, and 108), the fossil turtle *Proganochelys* (which is treated as the sister group to all other turtles) shares the character state with pleurodires rather than with cryptodires. Thus, it seems equally parsimonious to suggest that cryptodires simply retain ancestral morphological states and that pleurodires have derived ones. There also may be indirect support for this conjecture from the fossil record. The oldest known fossils assignable to essentially modern groups are from the Early Cretaceous about 110 million years ago: a trionychoid (*Sandownia harrisi*) from the Early Albian (Meylan et al., 2000), a chelonioid (*Santanachelys gaffneyi*) from the Late Aptian or Early Albian (Hirayama, 1998; Zangerl, 1953), and a pelomedusoid (*Araripemys barretoi*) from the Albian (Meylan, 1996). The almost simultaneous appearance of these three modern groups could be interpreted as a hard polytomy between trionychoids, non-trionychoid cryptodires, and pleurodires. Using a multi-calibration point molecular clock approach, Near et al. (2005) independently estimated an origination of pleurodires (176 million years ago), cryptodires (175 mya), and Trionychoidae (155 mya) that may be consistent with this scenario. This interpretation will be controversial, as some paleontologists consider the fossil *Proterochersis* from the Late Triassic (about the same age as *Proganochelys*) to be a pleurodire (Gaffney et al., 1991), implying that the Cryptodira–Pleurodira split dates to nearer the origin of turtles over 200 million years ago. Why disparate datasets should be harmonious across the majority of extant turtle phylogeny but conflict at the base of this tree is puzzling.

4.3. Broader implications

Besides various evolutionary issues specific to turtles, the results of our research have ramifications for morphology and paleontology, and the conciliation of data deriving from those fields and from molecular techniques. First and foremost, this study should not be read as a criticism of morphological and paleontological research. Indeed, the vast majority of our molecular phylogenetic results accord with those obtained from these valuable, longstanding fields of inquiry (see also Shaffer et al., 1997). Instead, we view our molecular study as providing a complementary perspective on phylogenetic relationships inferred from morphological characters, including novel insight into areas where character homology may be questionable and where rates of DNA sequence evolution can aid interpretation of branching patterns.

Our findings also shed light on important differences among analytical methods for estimating phylogenetic relationships. At the deepest phylogenetic level among extant turtle groups, MP, ML, and Bayesian methods produced different results. That such methods may yield discordant outcomes is not news (e.g., Huelsenbeck, 1995); however, it is especially disturbing here because the molecular properties of RAG-1 implied that the gene exhibited outstanding characteristics for phylogenetic analysis (Naylor and Brown, 1998; Sanderson and Shaffer, 2002). RAG-1 in turtles possesses no saturation, low base composition bias, and a homogeneous base composition. Despite these molecular properties, the analytical methods produced different phylogenetic answers. Perhaps it is simply too much to ask one gene to resolve a phylogeny spanning the time of turtles, at all depths in the tree. Regardless, we clearly need improved models of molecular evolution to reconstruct phylogenetic relationships using DNA sequence data.

Turtles represent one of the most recognizable radiations of life. As indicated by the fossil record, their unique Bauplan has remained largely unchanged for over 200 million years (Ernst and Barbour, 1989; Gaffney, 1990). Still, extant groups exhibit phenotypic variation that can shed light on important biological issues. For example, turtles exhibit a stunning diversity of sex-determining mechanisms (Janzen and Krenz, 2004, and unpublished results) and skull morphologies (Claude et al., 2004); unraveling their evolutionary tempo depends crucially on a well-resolved phylogeny. Our phylogenetic analyses of turtles thus provide a framework from which to launch highly informed comparative research in this remarkable group.

Acknowledgments

Julie Ryburn was especially helpful and patient with assistance in early molecular work. Dave Starkey in the Shaffer laboratory kindly located and supplied most of the tissues used in this study. James Parham was instrumental in locating key literature regarding *Platysternon*. David Weisrock, Allan Larson, and two anonymous reviewers provided critical comments on the manuscript. This research was supported by a Theodore Roosevelt Memorial Fund Grant from the American Museum of Natural History (J.G.K.), a Grant-in-Aid of Research from Sigma Xi (J.G.K.), and NSF Grants DEB-9629529 and DEB-0089680 (F.J.J.). J.G.K. was also supported by fellowships from the Graduate College and the Ecology and Evolutionary Biology Program at Iowa State University. The manuscript was completed while F.J.J. was a courtesy research associate in the Center for Ecology and Evolutionary Biology at the University of Oregon.

References

Bernstein, R.M., Schluter, S.F., Bernstein, H., Marchalonis, J.J., 1996. Primordial emergence of the recombination activating gene 1 (RAG1): sequence of the complete shark gene indicates homology to microbial integrases. Proc. Natl. Acad. Sci. USA 93, 9454–9459.

Bickham, J.W., Carr, J.L., 1983. Taxonomy and phylogeny of the higher categories of cryptodiran turtles based on a cladistic analysis of chromosomal data. Copeia 1983, 918–932.

Carlson, L.M., Oettinger, M.A., Schatz, D.G., Masteller, E.L., Hurley, E.A., McCormack, W.T., Baltimore, D., Thompson, C., 1991. Selective expression of RAG-2 in chicken B cells undergoing immunoglobulin gene conversion. Cell 64, 201–208.

Chen, B.-Y., Mao, S.-H., Ling, Y.-H., 1980. Evolutionary relationships of turtles suggested by immunological cross-reactivity of albumins. Comp. Biochem. Physiol. B 66, 421–425.

Claude, J., Pritchard, P.C.H., Tong, H., Paradis, E., Auffray, J.-C., 2004. Ecological correlates and evolutionary divergence in the skull of turtles: a geometric morphometric assessment. Syst. Biol. 53, 933–948.

Dalton, R., 2003. Mock turtles. Nature 423, 219–220.

Danilov, I., 1998. Phylogenetic relationships of platysternid turtles. In: Third Asian Herpetological Meeting Abstracts, p. 14.

Dumeril, A.M.C., 1806. Zoologie Analytique, ou Methode Naturelle de Classification des Animaux, Allais Libraire, Paris.

Dumeril, A.M.C., Bibron, G., 1835. Erpetologie General ou Histoire Naturelle Complete des Reptiles, Paris.

Engstrom, T.N., Shaffer, H.B., McCord, W.P., 2004. Multiple data sets, high homoplasy, and the phylogeny of softshell turtles (Testudines: Trionychidae). Syst. Biol. 53, 693–710.

Ernst, C.H., Barbour, R.W., 1989. Turtles of the World. Smithsonian Institution Press, Washington, DC.

Felsenstein, J., 1985. Confidence limits on phylogenies: an approach using the bootstrap. Evolution 39, 783–791.

Frair, W., 1972. Taxonomic relationships among chelydrid and kinosternid turtles elucidated by serological tests. Copeia 1972, 97–108.

Frair, W., 1983. Serological survey of softshells with other turtles. J. Herpetol. 17, 75–79.

Fujita, M.K., Engstrom, T.N., Starkey, D.E., Shaffer, H.B., 2004. Turtle phylogeny: insights from a novel nuclear intron. Mol. Phylogenet. Evol. 31, 1031–1040.

Gaffney, E.S., 1975. A phylogeny and classification of the higher categories of turtles. Bull. Am. Mus. Nat. Hist. 155, 387–436.

Gaffney, E.S., 1984. Historical analyses of theories of chelonian relationship. Syst. Zool. 33, 283–301.

Gaffney, E.S., 1990. The comparative osteology of the Triassic turtle *Proganochelys*. Bull. Am. Mus. Nat. Hist. 194, 1–263.

Gaffney, E.S., Meylan, P.A., 1988. A phylogeny of turtles. In: Benton, M.J. (Ed.), The Phylogeny and Classification of Tetrapods. Clarendon Press, Oxford, pp. 157–219.

Gaffney, E.S., Meylan, P.A., Wyss, A.R., 1991. A computer assisted analysis of the relationships of the higher categories of turtles. Cladistics 7, 313–335.

Gibbons, J.W., Scott, D.E., Ryan, T.J., Buhlmann, K.A., Tuberville, T.D., Metts, B.S., Greene, J.L., Mills, T., Leiden, Y., Poppy, S., Winne, C.T., 2000. The global decline of reptiles, déjà vu amphibians. BioScience 50, 653–666.

Groth, J.G., Barrowclough, G.F., 1999. Basal divergences in birds and the phylogenetic utility of the nuclear RAG-1 gene. Mol. Phylogenet. Evol. 12, 115–123.

Haiduk, M.W., Bickham, J.W., 1982. Chromosomal homologies and evolution of testudinoid turtles with emphasis on the systematic placement of *Platysternon*. Copeia 1982, 60–66.

Hirayama, R., 1998. Oldest known sea turtle. Nature 392, 705–708.

Huelsenbeck, J.P., 1995. Performance of phylogenetic methods in simulation. Syst. Biol. 44, 17–48.

Huelsenbeck, J.P., Ronquist, F., 2001. MRBAYES: Bayesian inference of phylogeny. Bioinformatics 17, 754–755.

Janzen, F.J., Krenz, J.G., 2004. Phylogenetics: which was first, GSD or TSD?. In: Valenzuela, N., Lance, V.A. (Eds.), Temperature-dependent Sex Determination in Vertebrates. Smithsonian Books, Washington, DC, pp. 121–130.

Klemens, M.W., 2000. Turtle Conservation. Smithsonian Institution Press, Washington, DC.

Kraus, F., Miyamoto, M.M., 1991. Rapid cladogenesis among the pecoran ruminants: evidence from mitochondrial DNA sequences. Syst. Zool. 40, 117–130.

Larson, A., 1994. The comparison of morphological and molecular data in phylogenetic systematics. In: Schierwater, B., Streit, B., Wagner, G.P., DeSalle, R. (Eds.), Molecular Ecology and Evolution: Approaches and Applications. Birkhäuser, Basel, pp. 371–390.

Li, W.-H., 1997. Molecular Evolution. Sinauer, Sunderland, MA.

Madsen, O., Scally, M., Douady, C.J., Kao, D.J., DeBry, R.W., Adkins, R., Amrine, H.M., Stanhope, M.J., de Jong, W.W., Springer, M.S., 2001. Parallel adaptive radiations in two major clades of placental mammals. Nature 409, 610–614.

Maisey, J.G., Naylor, G.J.P., Ward, D.J., 2004. Mesozoic elasmobranches, neoselachian phylogeny and the rise of modern neoselachian diversity. In: Arratia, G., Tintori, A. (Eds.), Mesozoic Fishes 3. Systematics Paleoenvironments and Biodiversity. Verlag. F. Pfeil., Munchen, Germany, pp. 17–56.

Meylan, P.A., 1996. Morphology and relationships of the early Cretaceous side-necked turtle, *Araripemys barretoi* (Testudines: Pelomedusoides: Araripemydidae) from the Santana Formation of Brazil. J. Vert. Paleontol. 16, 20–33.

Meylan, P.A., Moody, R.J.T., Walker, C.A., Chapman, S.D., 2000. *Sandownia harrisi*, a highly derived trionychoid turtle (Testudinata: Cryptodira) from the Early Cretaceous of the Isle Of Wright, England. J. Vert. Paleontol. 20, 522–532.

Murphy, W.J., Eizirik, E., Johnson, W.E., Zhang, Y.P., Ryder, O.A., O'Brien, S.J., 2001. Molecular phylogenetics and the origin of placental mammals. Nature 409, 614–618.

Naylor, G.J.P., Brown, W.M., 1998. Amphioxus mitochondrial DNA, chordate phylogeny, and the limits of inference based on comparisons of sequences. Syst. Biol. 47, 61–76.

Near, T.J., Meylan, P.A., Shaffer, H.B., 2005. Assessing concordance of fossil calibration points in molecular clock studies: an example using turtles. Am. Nat. 165, 137–146.

Orr, H.A., 2005. The probability of parallel evolution. Evolution 59, 216–220.

Posada, D., Crandall, K.A., 1998. Modeltest: testing the model of DNA substitution. Bioinformatics 14, 817–818.

Rambaut, A., 1995. Sequence Alignment Program v1.d1, University of Oxford.

Rodriguez, F., Oliver, J.L., Marin, A., Medina, J.R., 1990. The general stochastic model of nucleotide substitution. J. Theor. Biol. 142, 485–501.

Sanderson, M.J., Shaffer, H.B., 2002. Troubleshooting molecular phylogenetic analyses. Annu. Rev. Ecol. Syst. 33, 49–72.

Schatz, D.G., Oettinger, M.A., Baltimore, D., 1989. The V(D)J recombination activating gene, RAG-1. Cell 59, 1035–1048.

Shaffer, H.B., Meylan, P., McKnight, M.L., 1997. Tests of turtle phylogeny: molecular, morphological, and paleontological approaches. Syst. Biol. 46, 235–268.

Shimodaira, H., Hasegawa, M., 1999. Multiple comparisons of log-likelihoods with applications to phylogenetic inference. Mol. Biol. Evol. 16, 1114–1116.

Swofford, D.L., 2001. PAUP*. Phylogenetic Analysis Using Parsimony (* and Other Methods). Version 4, Sinauer, Sunderland, MA.

Tamura, K., Nei, M., 1993. Estimation of the number of nucleotide substitutions in the control region of mitochondrial DNA in humans and chimpanzees. Mol. Biol. Evol. 10, 512–526.

Templeton, A.R., 1983. Phylogenetic inference from restriction endonuclease cleavage site maps with particular reference to the evolution of humans and the apes. Evolution 37, 221–244.

Townsend, T., Larson, A., Louis, E., Macey, J., 2004. Molecular phylogenetics of Squamata: the position of snakes, amphisbaenians, and dibamids, and the root of the squamate tree. Syst. Biol. 53, 735–757.

Weisrock, D.W., Janzen, F.J., 2000. Comparative molecular phylogeography of North American softshell turtles (*Apalone*): implications for regional and wide-scale historical evolutionary forces. Mol. Phylogenet. Evol. 14, 152–164.

Whetstone, K.N., 1978. Additional record of the fossil snapping turtle *Macroclemys schmidti* from the Marshland Formation (Miocene) of Nebraska with notes on interspecific skull variation within the genus *Macroclemys*. Copeia 1978, 159–162.

Williams, E.E., 1950. Variation and selection of the cervical central articulations of living turtles. Bull. Am. Mus. Nat. Hist. 94, 505–562.

Zangerl, R., 1953. The vertebrate fauna of the Selma Formation of Alabama. Part 3. The turtles of the family Protostegidae. Part 4. The turtles of the family Toxochelyidae. Fieldiana Geol. Mem. 3-4, 61–277.